July 1997 • NREL/SR-520-23262

The Improvement of Near-Term CdTe Processing and Product Capabilities and Establishment of Next-Generation CdTe Technology

Annual Technical Progress Report 1 September 1995 - 31 August 1996

J. Kester and S. Albright
Golden Photon, Inc.
Golden, Colorado

National Renewable Energy Laboratory
1617 Cole Boulevard
Golden, Colorado 80401-3393
A national laboratory of
the U.S. Department of Energy
Managed by Midwest Research Institute
for the U.S. Department of Energy
under Contract No. DE-AC36-83CH10093

NREL/SR-520-23262 • UC Category: 1263

The Improvement of Near-Term CdTe Processing and Product Capabilities and Establishment of Next-Generation CdTe Technology

Annual Technical Progress Report 1 September 1995 - 31 August 1996

J. Kester and S. Albright
Golden Photon, Inc.
Golden, Colorado

NREL technical monitor: H.S. Ullal

National Renewable Energy Laboratory
1617 Cole Boulevard
Golden, Colorado 80401-3393
A national laboratory of
the U.S. Department of Energy
Managed by Midwest Research Institute
for the U.S. Department of Energy
under Contract No. DE-AC36-83CH10093

Prepared under Subcontract No. ZAF-5-14142-06
July 1997

NOTICE

Available to DOE and DOE contractors from:
Office of Scientific and Technical Information (OSTI)
P.O. Box 62
Oak Ridge, TN 37831
Prices available by calling (423) 576-8401

Available to the public from:
National Technical Information Service (NTIS)
U.S. Department of Commerce
5285 Port Royal Road
Springfield, VA 22161
(703) 487-4650

Phase One

ZAF-5-14142-06

Acknowledgments

GPI would like to thank all the folks at NREL that helped us. Technical Support was provided in the area of characterization and measurement by Rick Matson, David Niles, Dean Levi, Brian Keys, Dick Arhenkeil, Tim Gessert, Keith Emery, and Amy Franz-Schwartzlander. We would also like to acknowledge the perseverance of Harin Ullal and Ken Zweibel.

List of Contributors

John J. Kester
Scot P. Albright
Terry Brog
Victor Kaydanov
Larry Woods
Rosine Riblien
Jeff Phillips
Sean Sullivan
Neil Heeke
Don Morgan
Steve Carol
Bruce Walters

Summary

1. Demonstrated 29.3 watt 2' x 2' module - aperature area efficiency 8.8%, active area efficiency 10.5% - excellent stability.

2. Improved CdTe Morphology through recrystallization demonstrated by efficiency and stability.

3. Reduced production costs - reduced weight, thickness of module and permeability to water.

4. Modified graphite and dopant incorporation - demonstrated greater efficiency, uniformity, and reproducibility.

5. Participated in Team efforts

   - provided samples for CdS thickness/Voc testing
   - distributed CdTe material for back contact
   - development of Performance Certification Standardization

6. Provided modules to NREL of efficiency and life testing data.

List of Figures

List of Tables

Table of Contents

1.0 Introduction

The potential of photovoltaics to become a major global business enterprise still lingers outside the limits of industrial capabilities. For the Cadmium Sulfide/ Cadmium Telluride (CdS/CdTe) system this potential has continued to focus on improvements in efficiency, stability, and cost reduction. This triad is the primary objective of the present subcontract with NREL entitled "The Improvement of Near-term CdTe Processing and Product Capabilities & Establishment of Next Generation CdTe Technology". This subcontract represents an intermediate stage of NREL's plan to assist the growth of the photovoltaic industry in overcoming the scientific and technical barriers to commercialization. This report outlines the progress that has been made during the period of August 1995 through August 1996.

The objectives of this subcontract are to improve processing methods, quantify and understand efficiency improvement mechanisms, meet life-testing goals, and address cadmium safety concerns. Task and subtask goals are defined to meet these objectives in specific areas. The approach to fulfilling the subcontract goals is through a balanced plan of process improvement and mechanism identification. These are carried out and continued through monitoring under various long term and accelerated stress conditions. GPI maintains an on-going awareness of all safety related issues, can in particular, those involving cadmium.

A significant change in our company structure occurred during this subcontract phase. A variability in the stability of modules during a manufacturing scale up resulted in a reduction in the workforce and redirection of almost all company efforts towards research and development issues and product certification This redirection has led to a substantial growth in the understanding of the connection between the morphological and electronic properties of this system. Significant improvements have been made in stability and efficiency subsequent to this redirection and are outlined below. As well as these improvements, cost reduction was realized in the area of module encapsulation.

Achieving stability and efficiency goals during Phase II will poise GPI for a solidly-based re-entry into commercialization. Commensurate with these achievements are planned reductions in the manufacturing costs that will meet cost goals that will achieve sufficient market share. As these goals are met and a standard module design has been achieved, then additional efforts will need to be placed on the end-of-life recycling issues.

1.1 Background

This document is the Golden Photon, Inc. Phase One Annual report submitted to the National Renewable Energy Laboratory for the subcontract ZAF-5-14142-06. This subcontract was awarded to Golden Photon, Inc. to demonstrate near term progress in CdTe processing and product capabilities. This subcontract directly supports NREL's planned advancement of photovoltaic technology toward low cost commercialization goals. GPI has clearly shown this advancement by the progress demonstrated in the previous subcontract, # ZN-0-19019, through improvements in efficiency as well as increasing the module size by a factor of 4.[1]

Photon Energy, Inc. was acquired and renamed Golden Photon, Inc. in 1992 by ACX Technologies Incorporated. GPI was relocated to Golden, Colorado from El Paso, TX. The new facility allowed the upgrade to a full proto-type 2 megawatt facility which began production of 2' x 2' modules in late 1993. The facility planned for growth of the manufacturing process through a combination of a fully functional manufacturing process and research and development effort. Tremendous progress was made with the manufacture of 12.3% efficiency cells with open circuit voltages(Voc) of 0.78 volts and short circuit current densities (Isc) of 25.0 ma/cm^2 .

1.2 Status of the Facility

GPI's facility comprises 30,000 square feet within the Golden Technologies headquarters. This facility includes the manufacturing production lines, research and development, process and environmental control, encapsulation, and testing areas. Despite the reduction in manpower over the past year, GPI retains the utilization of all the existing capabilities that were in place and has even expanded those capabilities to allow more in-depth understanding of processes and testing.

The testing capabilities of GPI were expanded during the past year. The outdoor testing facility was expanded to allow for greater than 400 full size modules to be deployed. In addition, this array has radiometric and meteorologic facilities which are computer interfaced for continuous tracking.
An indoor array was assembled for 24 hour exposure of modules. The correlation of results from the indoor array will be compared with results of outdoor testing to establish this method as an accelerated test capability. Additional facilities for testing devices and modules under elevated temperature, voltage bias, ultraviolet and visible irradiation were put into place and utilized.

An upgrade of measurement capabilities was implemented during Phase one of this subcontract. GPI acquired a Quadtech Inductance-Capacitance-Resistance bridge for measurement of cell capacitance and sheet resistance samples. This bridge was used in combination with a voltage source and digital voltmeter to access a wide range of applied voltages and to the device. These instruments were all interfaced under IEEE-488 through a Labview program to provide a versatile testing of materials. In addition to the measurement of capacitance versus voltage the program calculates the carrier concentration as a function of depth from the junction of the device. Results of testing performed with this equipment are discussed in a later section.

Another improvement in process control was incorporated into the CdS thickness measurement. A time intensive technique was replaced with the help of researchers from NREL by an optical measurement process. Through the use of frequency dependent optical transmission the thickness of CdS can be accurately and reproducibly measured. This technique allows rapid determination of film thickness and on-line control of the production process.

During Phase one of this subcontract a new research and development production capability was initiated. This capability will allow the deposition of all device layers in a fashion similar to that done on the full scale production facility but on a smaller size. This off-line production facility will allow for faster testing of parametric relationships. The off-line facility will have the

capability of precise temperature, air flow, deposition parameters that will decrease variability and allow for accurate correlation with cell parameters. This new capability will be brought on line during the next Phase of this subcontract.

2.0 Status of Development

The meter stick of commercial development measures progress in photovoltaics by improvements in efficiency, stability, and production cost. The relative value of each of these parameters are determined by the particular market need that is being filled. GPI has made significant progress in each of these areas over the past year. The progress that has been demonstrated is based on a greater depth of understanding of the electronic processes and the dependence of these processes on the composition and morphology of the material.

Clearly the primary efficiency goal of a developmental manufacturing facility is the optimization of production line fabrication to produce the highest power output of modules. The fabrication of small area devices is of importance only from the standpoint of a target efficiency achievable on the production line. To eliminate as many differences between standard production of the base material and laboratory material, all tests utilize material produced as far along the production process as possible. After extraction from the production line small area devices are completed using processes as close to the production facility as possible.

2.1 Efficiency

Improvements in uniformity of panels has allowed the production of good efficiency cells using material which had all the films deposited on the manufacturing line. A typical cell is shown in Figure 1. This 12.2% efficiency device has an area of approximately 0.3 cm^2. Small cells of this efficiency can be made routinely using standard films produced on the manufacturing line. The highest efficiency cells (not confirmed at NREL) have efficiencies greater than 13%. The open circuit voltage of the cell in Figure 1. is 792 millivolts and short circuit current density is 24.2 mA/cm^2. The relative quantum efficiency of this device is shown in Figure 2. The current density observed in this cell is enhanced by the increased response at wavelengths shorter than the CdS cutoff near 500 nm.[2] This response is an indication of thin CdS layer in our device. As will be discussed later this is due to diffusion of CdS into the CdTe layer. In addition to the enhanced UV response, this diffusion results in an alloy of CdTe with a band edge at longer wavelengths. The 50% level on the relative quantum efficiency curve is near 855 nm. This extension of the band edge enhances the current collection in the near -IR region.

The improvement in efficiency of the devices described above has been translated into high efficiency modules. Figure 3. shows the IV characteristics of a 2' by 2' module after 75 days on GPI's outdoor array. The maximum power output was 29.3 watts when normalized to 1000 $watts/m^2$. The fill factor was approximately 60%. The total area (3755 cm^2) efficiency of this module is 7.8%, the aperture area (3350 cm^2) efficiency is 8.7%, and the active area efficiency is 10.5%. The 16% difference between aperture and active areas is due to the large area loss due to our current division process. The reduction in division losses is a goal for the next phase of this

subcontract. A reduction of the division losses by only 25% would allow GPI to exceed the world record total area efficiency of 9.1% for CdTe modules greater than 1 sq. ft. (Ref.3) The active area efficiency of this module is already a world record for CdTe.

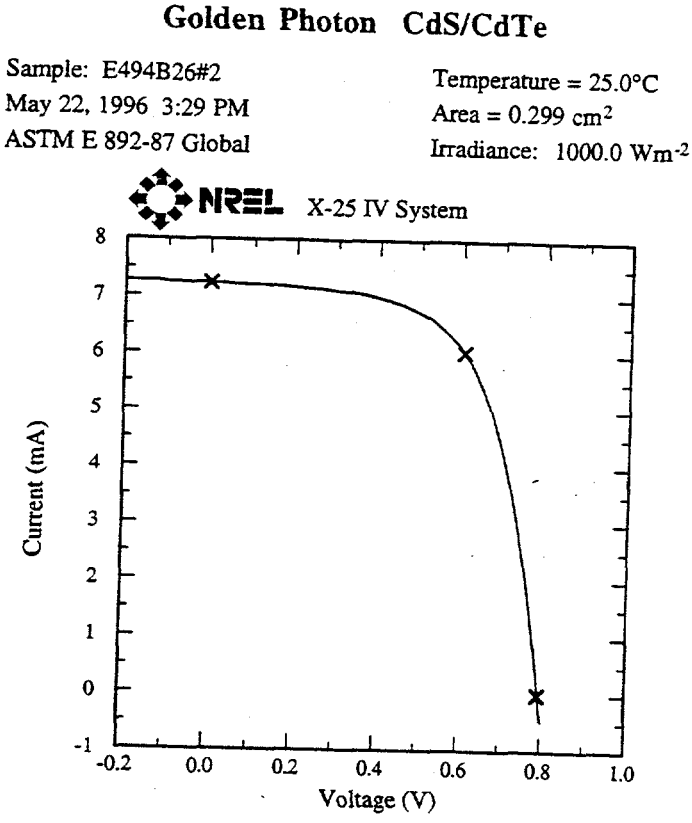

V_{oc} = 0.7926 V
I_{sc} = 7.228 mA
J_{sc} = 24.18 mAcm^{-2}
Fill Factor = 63.69 %

V_{max} = 0.6044 V
I_{max} = 6.038 mA
P_{max} = 3.649 mW
Efficiency = 12.2 %

After 10 minute soak @ P_{max}., 2 minute cool.
Current collection outside metal back contact

Figure 1. Current vs. Voltage of a typical GPI cell measured at NREL, including cell parameters

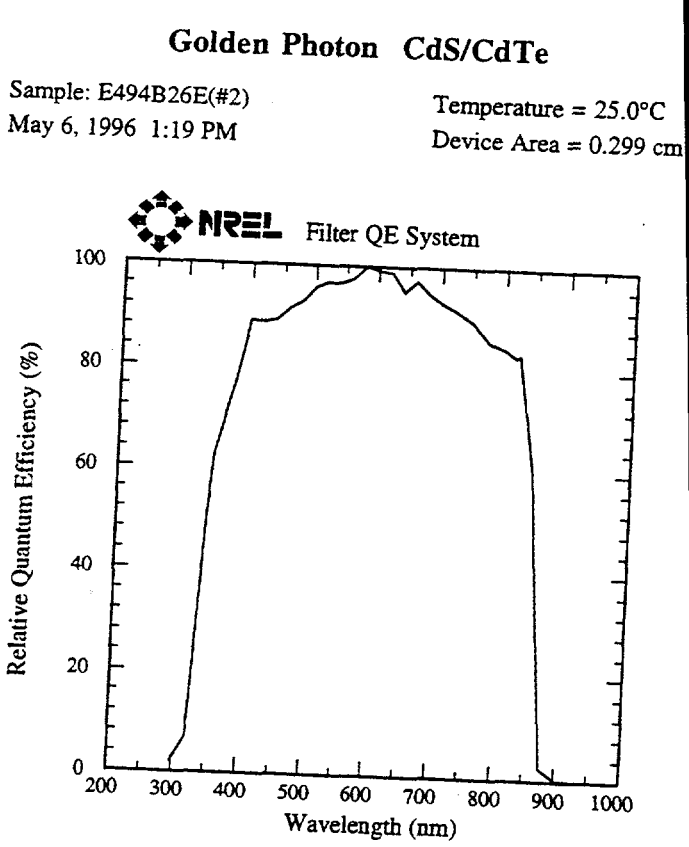

Light bias = 3.00 mA
Bias Voltage = 0.00 V

Figure 2. Quantum efficiency vs wavelength of the cell in Figure 1.

Golden Photon CdS/CdTe Module

Sample: 587-17
Nov 4, 1996 11:44 AM MST
device Temperature = 22.2°C

area used = 3492.8 cm2
1033.3W/m^2 fixed tilt
Si Ref. cell #294278

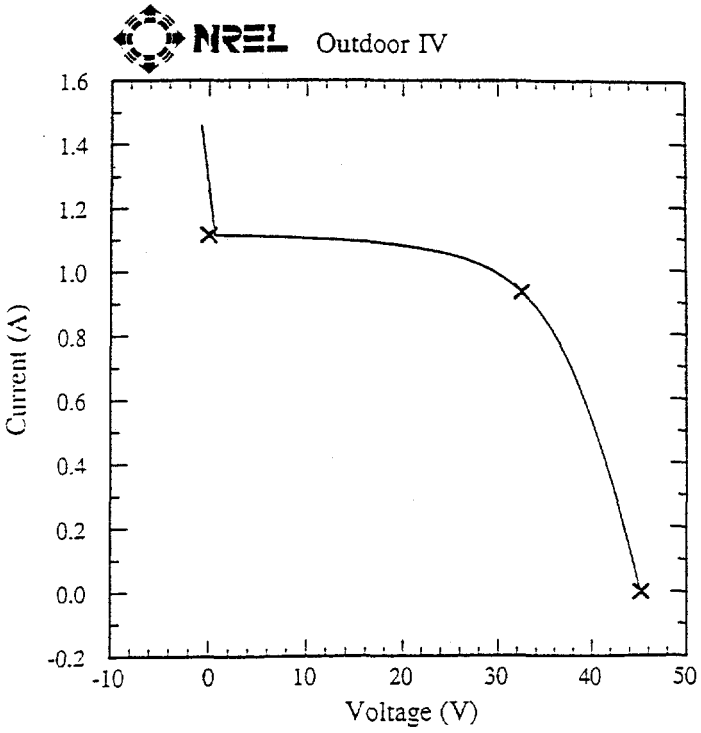

V_{oc} = 45.17 V
I_{sc} = 1.117 A
Fill Factor = 59.97 %
Efficiency = 8.38 %

V_{max} = 32.45 V
I_{max} = 0.9325 A
P_{max} = 30.26 W

59.2x59.0 cm aperture
part of GP stability study
Air temperature = 14.5°C, Air mass = 1.75, POA sun angle = 25.0°

Figure 3. Current vs. Voltage of 2' by 2' module after 75 days on GPI's outdoor array. Normalized Pmax=29.3 watts

2.2 Stability

The stability of modules, submodules, and small cells have been measured under different testing conditions, including, illumination, temperature, and voltage bias. The majority of testing on full size modules is done on GPI's outdoor array. These panels are resistively loaded to their maximum power point. Panels removed from the array for testing are allowed to equilibrate to the typical building temperature of 24°C -27°C. Panels that are placed in non-standard conditions; UV illumination, elevated temperature in the dark or light, or under forward or

reverse bias, are placed outside for a period of four hours to remove any artifact that the non-standard conditioning may have produced in the module.[2]

The use of small cells allows for the testing of multiple parametric relationships and larger statistical measures without taking up significant amounts of space on our outdoor array. Small cells can be sealed within a structure that has the same encapsulation materials and techniques as a full size panel. These encapsulated cells are then placed in the same testing conditions as full size modules. The use of small cells also allows us to more accurately test other properties of cells, such as, capacitance and quantum efficiency.

A series of six modules was delivered to NREL during Phase one. These modules had been on GPI's outdoor array for time periods of two weeks to almost one year. One of the longer term modules is shown in Figure 4. The linear least squares fitting of this data indicates a degradation rate of 0.4% per year. This module was measured at NREL three times over a period of six weeks and produced an average of 22.3 watts. The difference of approximately 10% between GPI measurements and NREL's outdoor measurements is due to the lack of UV intensity in GPI's indoor testing apparatus that appears to reduce the fill factor. Recent modules have shown continued improvement in wattage, such as, the 29.3 watt panel in Figure 3. This measurement was made at the end of a 75 day testing period which showed an average difference from the initial value of 2.1% which is comparable to our testing error. This data will be discussed later in the technical investigations section when compared with alternate processing techniques.

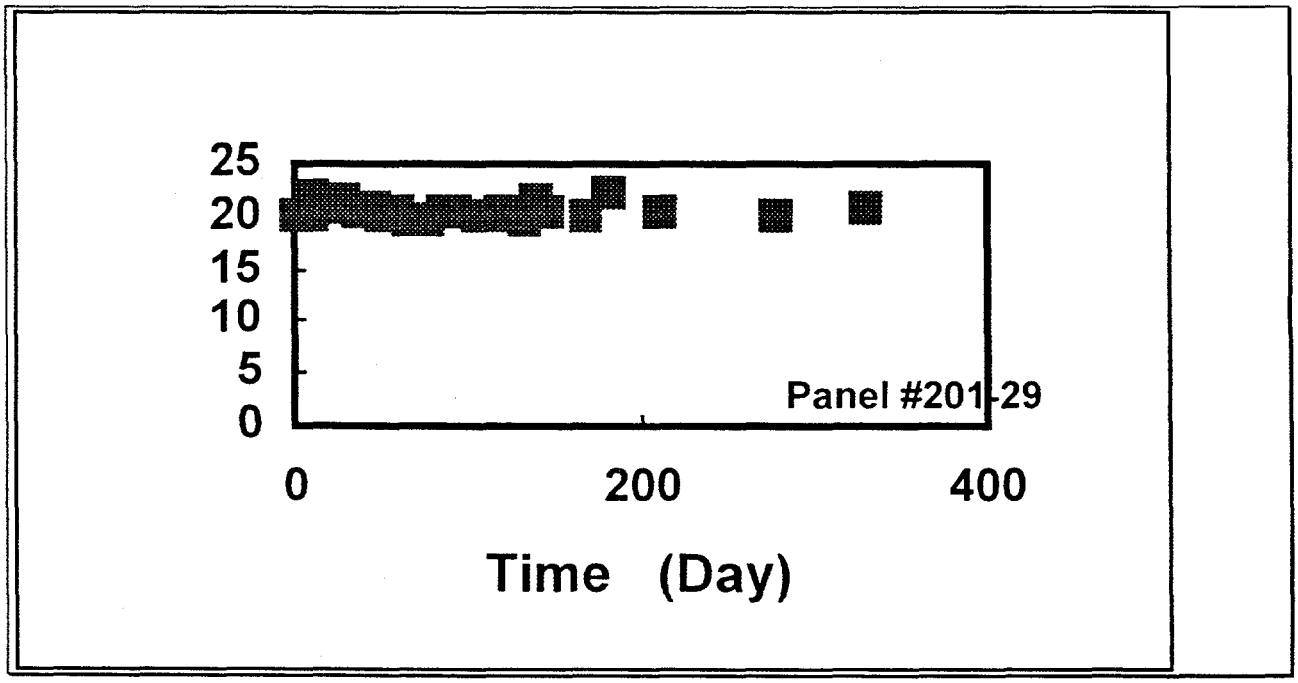

Figure 4. Power vs time of 2' by 2' module deployed on GPI's outdoor array. Panel delivered and tested at NREL after one year exposure measured 22.3 watts.

2.3 Uniformity and Reproducibility

Two important steps for any production process are uniformity and reproducibility of the product. For photovoltaic modules uniformity across a device is easier to attain if the production process is reproducible from panel to panel within a batch and among batches. Attaining correlations and controlling key product parameters at each process step panel is critical to the initiation of statistical process control. A key measure of overall process uniformity is the uniformity of cell parameters determined by current/voltage characteristics. This allows the separation of processing effects in the entire module (reproducibility) or specific areas of the module (uniformity). This technique has allowed GPI to identify problems at specific process steps by the location and symmetry of the variations across a panel.

Spatial variations in the panel characteristics allowed GPI to identify a non-uniformity in CdS thickness as a function of distance across the panel shown in Figure 5. This variation represented a 13% variation across the panel. When the CdS deposition process was corrected the resulting improvement in thickness uniformity is demonstrated by Figure 5. which shows a less than 3% variation.

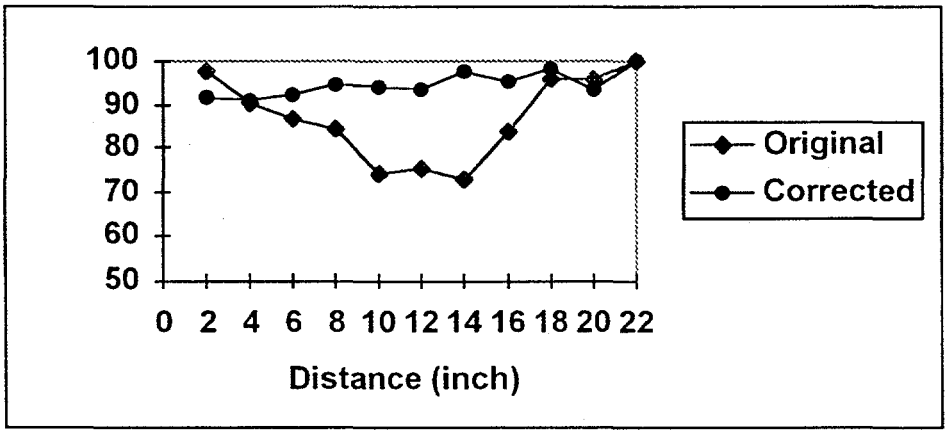

Figure 5. CdS thickness as a function of distance across a 2' x 2' panel before (diamond) and after (circle) correction of deposition spray profile.

The improvement of panel processing significantly improved the uniformity of panels. Figure 6. shows the efficiency as a function of position across the standard 2' x 2' panel. Each bar is the average of 4 cross cut cells with an area of approximately 0.8 cm^2. The average efficiency of cells across the panel is 10.3 % and the standard deviation is 4.6% of this value.

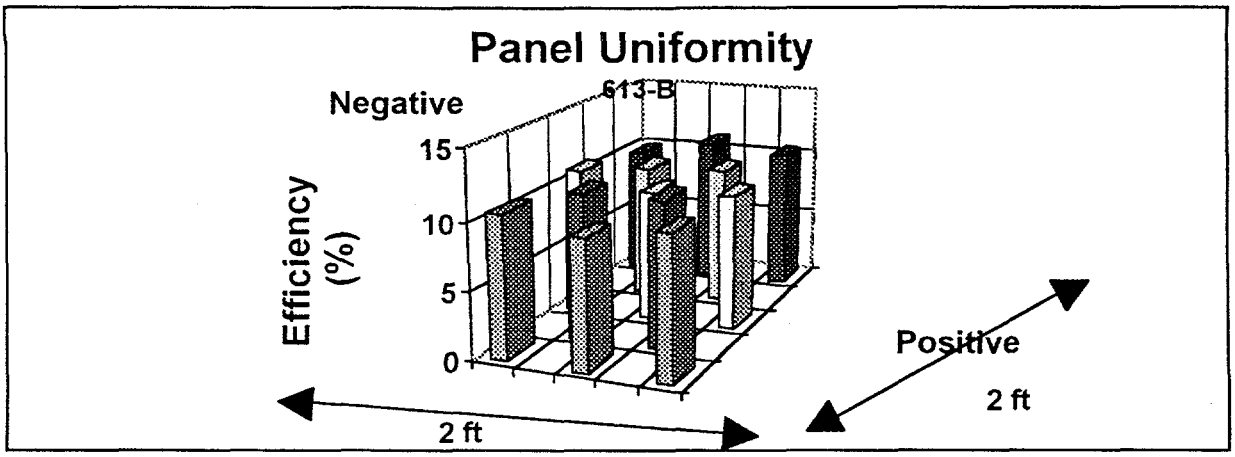

Figure 6. Efficiency of cells as a function of location across a 2' x 2' panel.

The ability to improve uniformity within a panel is a consequence of the improvement in reproducibility from panel to panel within a batch. Figure 7. shows the distribution of panel wattages within one batch of 41 modules. The panels show a distribution with over 90% of the modules within $\pm$ 1 watt of the mean.

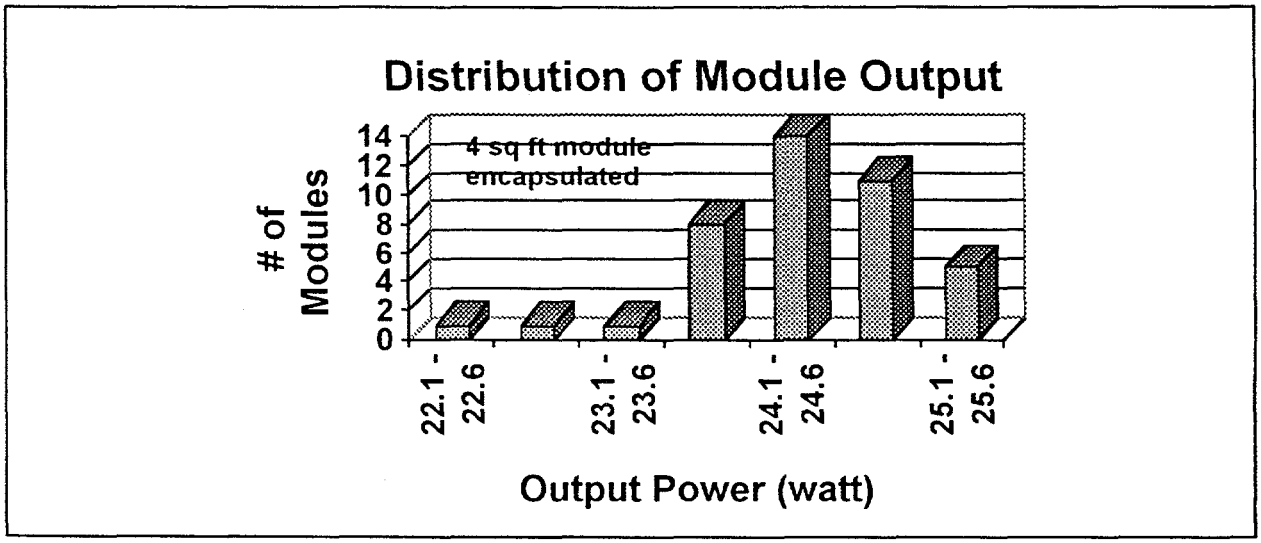

Figure 7. Distribution of the power of encapsulated modules comprising one batch.

The uniformity of the stability across a panel can also be tested. Before panels are encapsulated they can be further electrically isolated to allow for separate testing of different regions of the panel. One configuration divides the panel into 16 submodules without any separation of the different submodules from the original glass substrate. These submodule devices can each be wired and the entire panel encapsulated using standard processing techniques. Recent submodule panels show good uniformity of the stability across the panel.

2.4 Device structure

The current structure of GPI's device is shown in Figure 8. This structure is built on soda lime glass with a tin oxide layer having a sheet resistance of 10-12 ohms per square. This is followed by a patented high resistance tin oxide layer.[4,5] The semiconducting layers of CdS and CdTe are then indicated. The thickness of the CdS layer is indicated in the figure as a thin layer because of the high quantum efficiency observed in the wavelength range 350 to 500nm (Figure 2. above) where CdS is absorbing. The CdTe layer has two distinct morphological regions: one dense region near the CdS layer followed by a more porous CdTe structure. The back contact is made with graphite followed by tin. The material is interconnected with the standard scheme shown in Figure 9. This figure shows the standard daisy chain connection from the top of one cell defined by a conducting strip to the bottom of the next cell. As mentioned above the reduction of optical losses due to interconnection between cells is an engineering goal for the next phase of this subcontract.

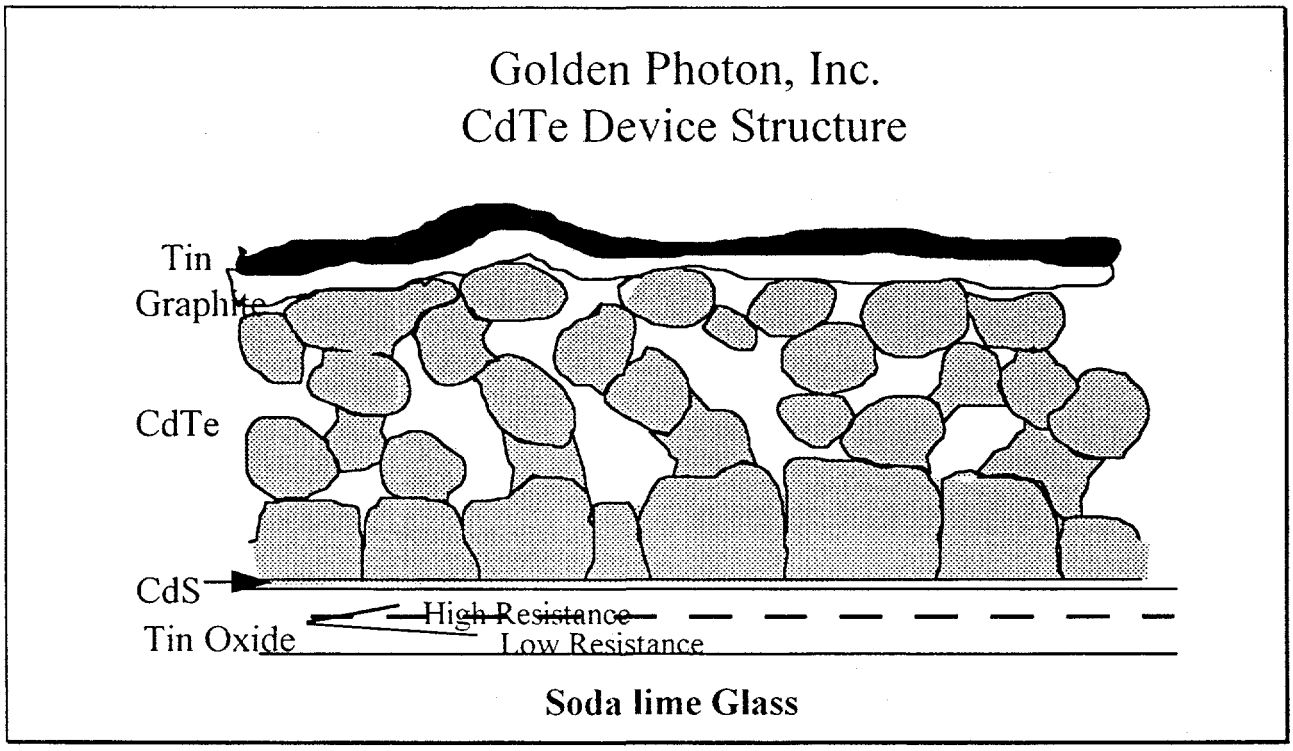

Figure 8. Model structure of GPI device.

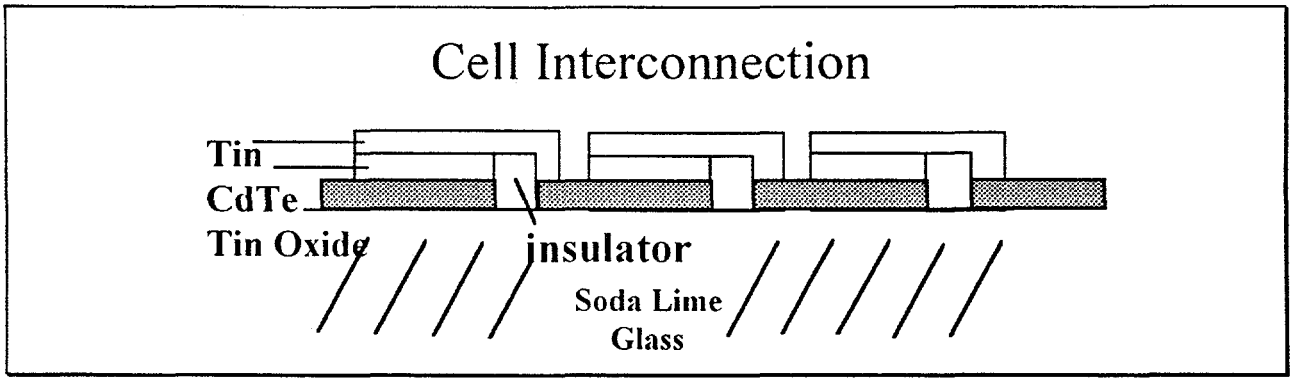

Figure 9. Model of interconnection of GPI cells on a module.

During this phase of the subcontract there was substantial improvement in module design. The improvements include the reduction in interior volume of an encapsulated panel. The reduction allowed GPI to eliminate an edge spacer and a sheet of filler glass between the front and back glass. The weight reduction improves handling and shipping issues. The decrease in the cross sectional area of the seal reduces the permeability of water. The side impact resistance of module was also improved by the installation of an edge protector around the entire module. The edge protector also eliminates the need for the large panel framing which was previously used. The improvements made in module encapsulation produced an additional advantage of cost reduction.

2.5 Qualification testing

The module design that was utilized for most of this subcontract period was initiated in 1992. This design had undergone and had substantially passed all of the IEEE25 Qualification Tests by July 1996 at Arizona State University under Bob Hammond with limited efficiency losses. UL representatives certified all the testing at ASU related to UL tests as satisfactory, with some residual issues with the junction box.

With the change in module design indicated in the preceding paragraphs requalification of the new design must be carried out. The improved module design is not believed to diverge substantially from the previous version and thus should not produce any problematic response to qualification testing. To date, GPI has completed the following tests on the new frameless/spacerless module.

Test	Test Location	Test Result
Hail Impact Test	ASU	Successful
Dynamic Loading	NREL	Successful
Twist Test	NREL	Successful
Dry Hi-Pot Test	GPI	Successful
Wet Hi-Pot Test	GPI	Successful
Thermal Cycling	GPI	Successful
Humidity Freeze		Not Done
Outdoor Exposure	GPI	In Process

Table 1. IEEE25 Qualification tests, test location, and test result

2.6 Environmental, Safety and Health

OSHA Related Issues

The OSHA Cadmium Standard is utilized at GPI's facility to steer all work with regard to a medical screening program, a cadmium compliance plan, an airborne cadmium sampling program, and a cadmium wipe sampling program. Medical and cadmium sampling records are being recorded to clarify the toxicity risks of working with cadmium and possibly other hazardous materials.

The GPI Environmental, Health, and Safety Plan includes occupational safety procedures, hazardous communications and training, updated active MSDS file, personal protective equipment (PPE) procedures, egress decontamination procedure, waste handling and disposal procedures, and training plans for the safe handling, storage and transfer of hazardous material. In the event of a release or spill and emergency response plan has been implemented.

Environmental Protection Issues

Air Emissions

Two EPA permitted dust collection systems are utilized to scrub all cadmium process exhausts. One system is designed to capture particulates only, while the second system captures the particulates as well as destroys volatile organic compounds. Each system contains two separate filter systems to provide secondary containment in case of a catastrophic failure of the primary filter. Both systems achieved capture efficiencies that have resulted in full compliance with legal requirements.

Water emissions

Water effluent is collected from each wet process in the facility. It is also collected from the standard plant cleaning work which is performed daily. A precipitation filtration method reduces cadmium concentrations to levels less than the legal limit. All treated waste water sample testing is performed by an independent certified laboratory.

Soil Emissions

The cadmium sampling plan listed above includes sampling points outside the production facility to certify that accumulation in the soil have not occurred.

Waste

A waste plan is in place to provide procedures and training for accumulating, permitted compacting, stabilization, temporary storage, and disposal of all waste streams generated at the facility. We are currently working with the Jefferson County (GPI's facility site) Department of Environment and Health and the DOE Climate Wise group on new methods of waste reduction and recycling. A contract presently allows us to recycle process fall off and scrap modules through Asarco in Helena, Montana.

GPI maintains awareness of results of the SBIR contracts for recycling of CdTe modules that is being conducted by Drinkard Research and Development Corporation and SCI.[6] The results of this work are the basis for planned recycling that must occur at the end of their 15 to 20 year life span.

3.0 Technical Investigations

3.1 Recrystallization

A key issue in the manufacture of photovoltaic devices of CdTe/CdS with high efficiency and long term stability is the morphology of the CdTe layer. Almost all manufacturing processes of CdTe cells include a heat treatment of the CdTe after its deposition which recrystallizes the CdTe producing an increase in grain size and homogeneity The structure of a device is shown in the scanning electron micrograph of Figure 10. This micrograph shows the layers described in Figure 8. above, however the CdTe region is divided into a dense region near the electronic junction followed by a porous region in contact with the graphite back electrode. The electronic properties of the resultant grain structure are highly dependent on the recrystallization parameters of temperature and time at temperature. The variability in stability observed on GPI modules up to mid-1996 have been identified and substantially solved by the improvement in the morphology of the CdTe.

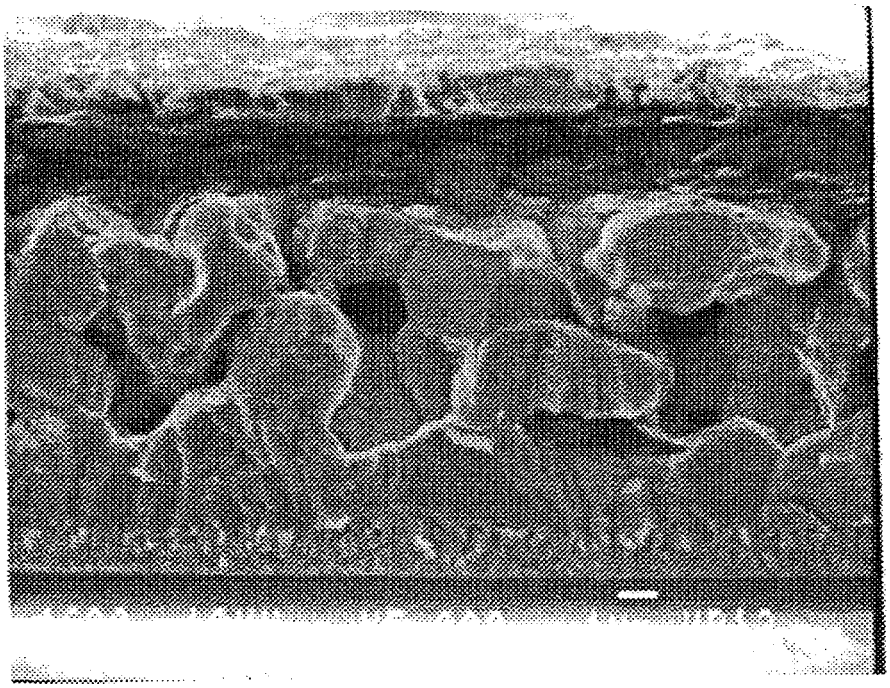

Figure 10. Scanning electron micrograph of GPI structure as illustrated in Figure 8. Small bar in the lower right shows 1.0 micron scale.

A significant improvement in cell parameters and stability has been produced by progress in the recrystallization of the CdTe film. The key parameters governing the recrystallization are the soak temperature and time at temperature. Changes in recrystallization are part of a multivariant parameter space that requires a re-optimization of other panel processes when recrystallization is modified. However critical sensitivities can be determined from a test of a single parameter. Figure 11. shows the percentage change versus time of outdoor testing for the module with P_{max} = 29.3 watt (Figure 3. above) in comparison with another from the same batch which had a

different time/temperature profile during recrystallization. Except for the change in recrystallization, all other film depositions and processing steps for these panels were identical. The change in the time/temperature profile produced 4 panels with less than 2.7% degradation from their initial values The old recrystallization process produced 4 modules with greater than 25% degradation. The primary cell parameter responsible for this degradation is series resistance.

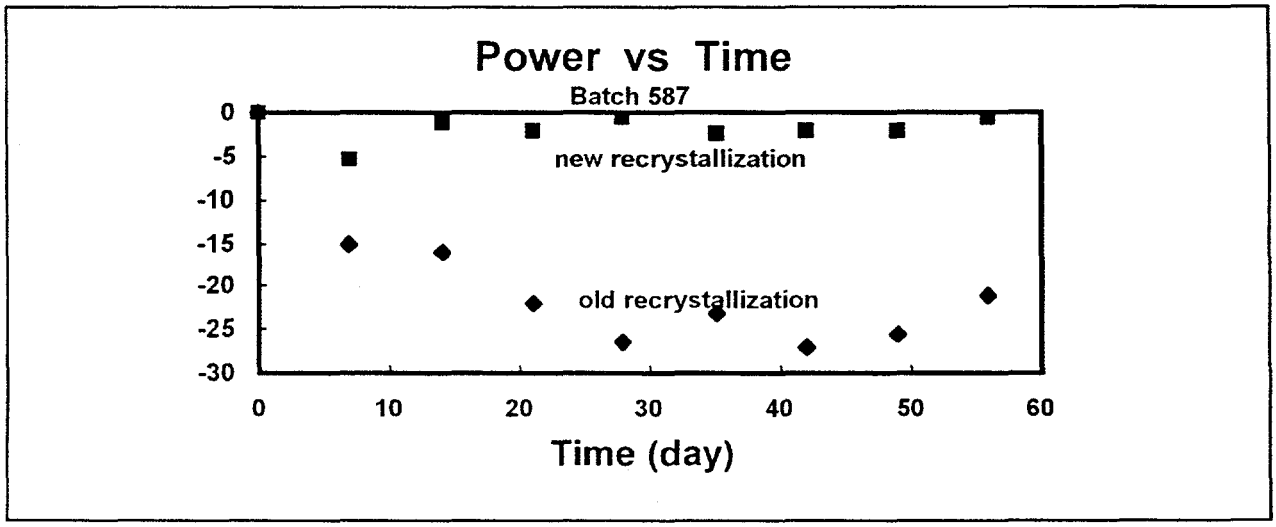

Figure 11. Power vs. Time of modules produced in by two different recrystallization methods.

The change in the time/temperature profile for CdTe recrystallization produces a dramatic change in morphology. The scanning electron micrograph (SEM) in Figure 12. compares the more stable CdTe material (Figure 12b.) with the less stable recrystallization (Figure 12a.). Examination of the SEM in Figure 12b. shows the improved time/temperature recrystallization profile has larger and more uniform grains than the old recrystallization profile in Figure 12a. The dense region of the improved recrystallized material is increased by over 20% in comparison with the old recrystallization procedure. The effect of this morphology on electronic properties is discussed in the next section.

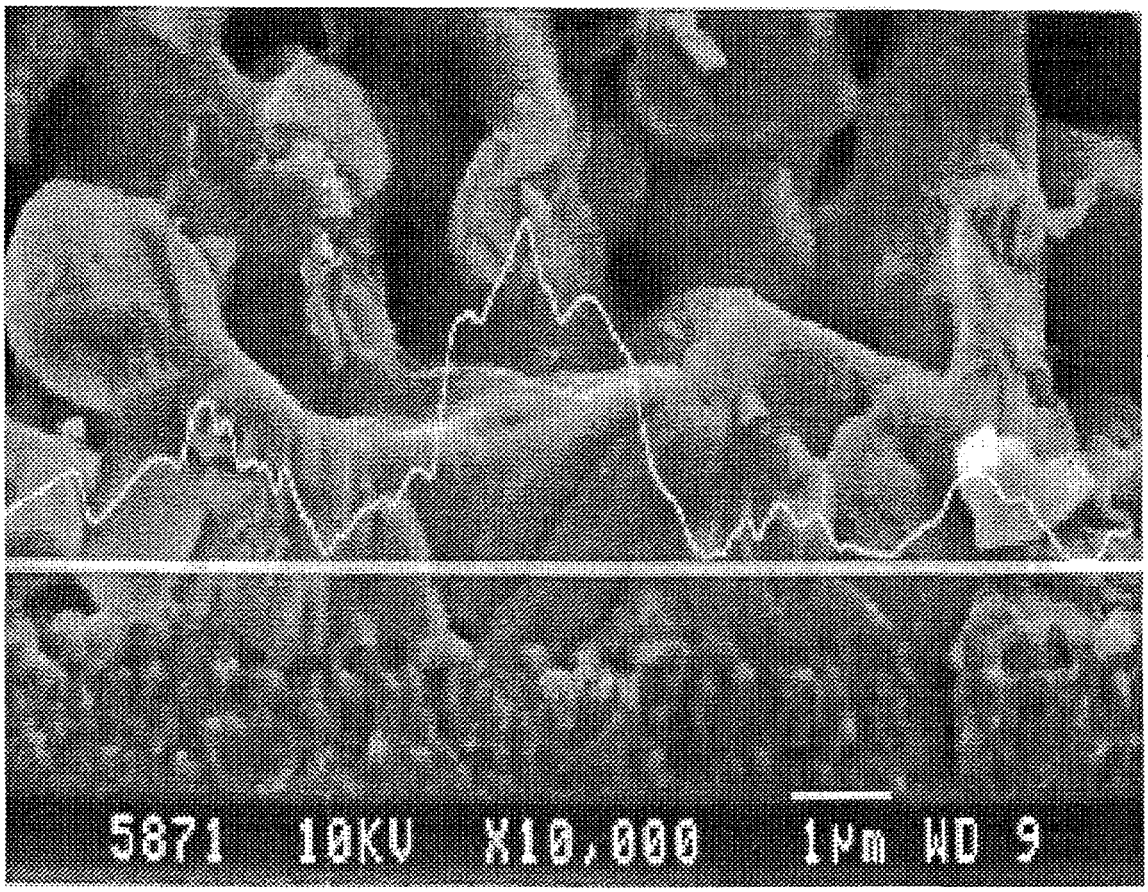

Figure 12a. Scanning electron micrograph of material with old (a) and new (b) recrystallization procedure.

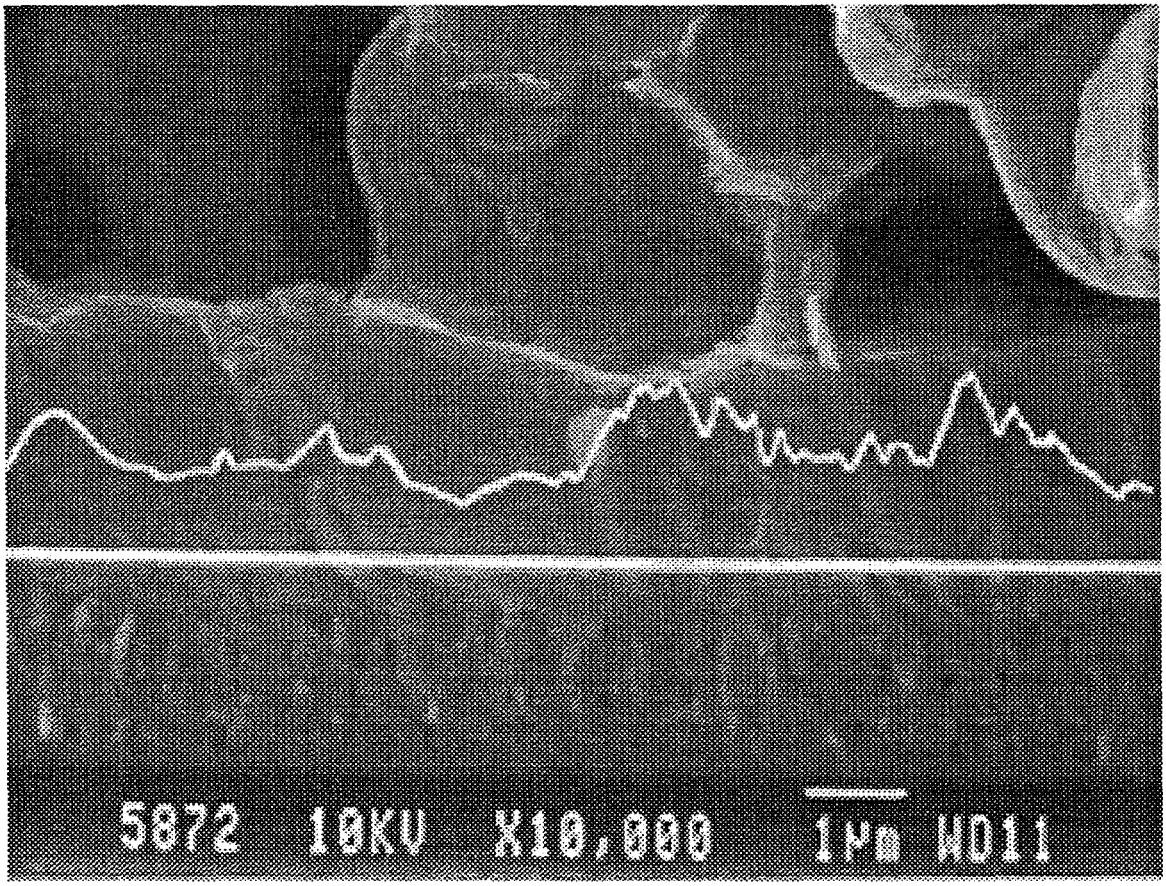

Figure 12b. Scanning electron micrograph of material with old (a) and new (b) recrystallization procedure.

Two primary modes of sintering of films are volume "solid state" diffusion and vapor phase transport (VPT).[7,8] Volume diffusion is characterized by densification and shrinkage of the material causing coalescence into a dense homogeneous structure. VPT increases particle size but with no large scale densification or removal of pores as evidenced by the material microstructure. The sintering of material by these two modes is illustrated in Figure 13. with a two sphere model. The volume diffusion shows a coalescence of the particles that will generally grow into a single sphere. The vapor transport mechanism fills in the neck region by evaporation from surface of the particle and condensation in the neck region where the local vapor pressure is higher. The changes observed in GPI material in Figures 10. and 12. are consistent with recrystallization that is dominated by vapor phase transport. The overall thickness of the layer is not substantially changed from before to after recrystallization. Within the porous region is evidence of transport to neck regions between particles that have growth at the expense of nearby smaller particles that volatilized.

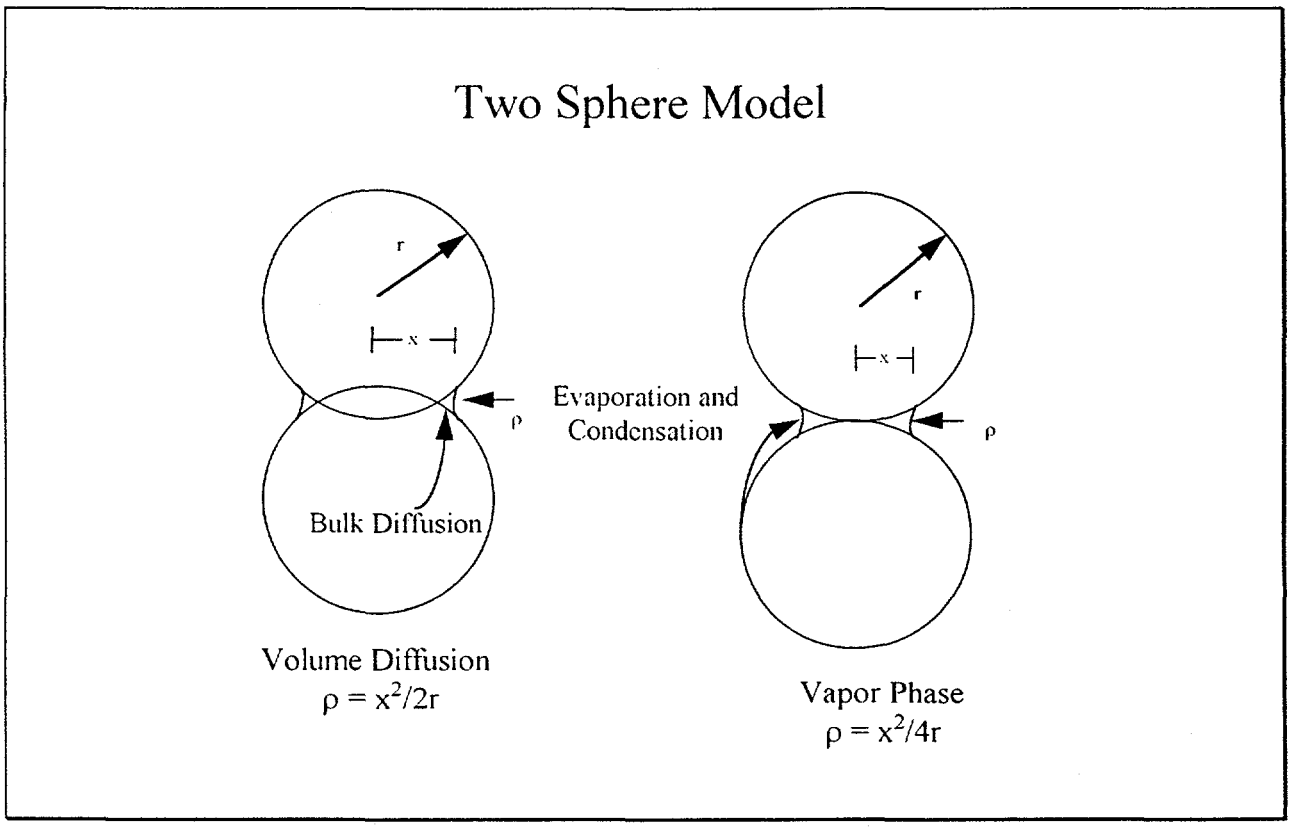

Figure 13. Model of two types of recrystallization of CdTe grains.

Additional testing has been carried out that indicates that the growth of the material is indeed dominated by VPT during recrystallization. Extended recrystallization processes display an asymptotic growth in particle size of CdTe without any reduction in the films total thickness or pore volume. Thermodynamic modeling has been carried out on systems approximating our recrystallization constituents. This modeling verifies the constituents have adequate vapor pressures at the temperatures employed to allow transport to occur. Further thermodynamic modeling will allow optimization of conditions which govern VPT and identify limits of densification.

3.2 Junction Effects

As discussed above the new recrystallization technique produces a larger dense region of CdTe and larger and fewer grains in the porous region of CdTe. In addition to these changes in morphology important changes were observed in the resultant electronic properties of the material. These changes were produced by a combination of morphology and the distribution of atomic constituents of the junction region. The distribution of material is also a function of this recrystallization process.

Figure 12. shows the electron beam induced current (EBIC) line scans along with the scanning electron micrographs of the regions from which they were taken. The EBIC line scans were taken within the CdTe along a line parallel to the junction region approximately one micron on the

CdTe side. The line scans indicate the collection efficiency of electrons injected into the device during the SEM process. This efficiency for the collection of these electron induced currents is proportional to that produced by optical generation of photocurrents during normal cell operation.

A comparison of the two types of recrystallization indicates that the new technique produces a more uniform collection efficiency than the older recrystallization profile. A digitization of the EBIC traces shows three times the standard deviation in photocurrent for the old crystallization above the new. While some of this variation is due to an interference by topographic features induced by fracturing, a comparison of the secondary electron images and the electron beam induced currents show that, while related, surface topography does not dominate the EBIC results.

In addition, the photoluminescence intensity at approximately 850 nm that is due to CdTe adjacent to the junction is greater for the new crystallization. This is consistent with a decreased dependence on surface or grain boundary states due to more uniform and increased grain sizes of the new recrystallization process.

3.3 Resistivity

Because of the device's stability dependence on its recrystallization procedure (Fig. 11) and because the stability performance over the first two months in the field is dominated by the series resistance, a correlation was sought between the CdTe sheet resistance and the series resistance of a device. CdTe films were produced in a manner similar to the production of CdTe in an active device. The films were produced in such a manner that only the porous structure of CdTe was obtained. The CdTe films were treated in a manner similar to GPI's standard device processing and electroding. The back contacts were again similar to our standard process. These contacts were placed in parallel lines with a spacing of 2 to 4 mm. Aspect ratio of the line length to line separation was always greater than 10.

A electrical model of the porous region of the CdTe layer is shown in Figure 14. The porous region includes intragrain resistances, R_1, separated by the grain boundaries which can be represented by a parallel resistance and capacitance, R_2 and C, respectively. The measured resistance, R_m, is therefore a function of frequency, ω, given by

$$R_m = R_1 + \frac{R_2}{1 + (R_2 C \omega)^2} \qquad (1)$$

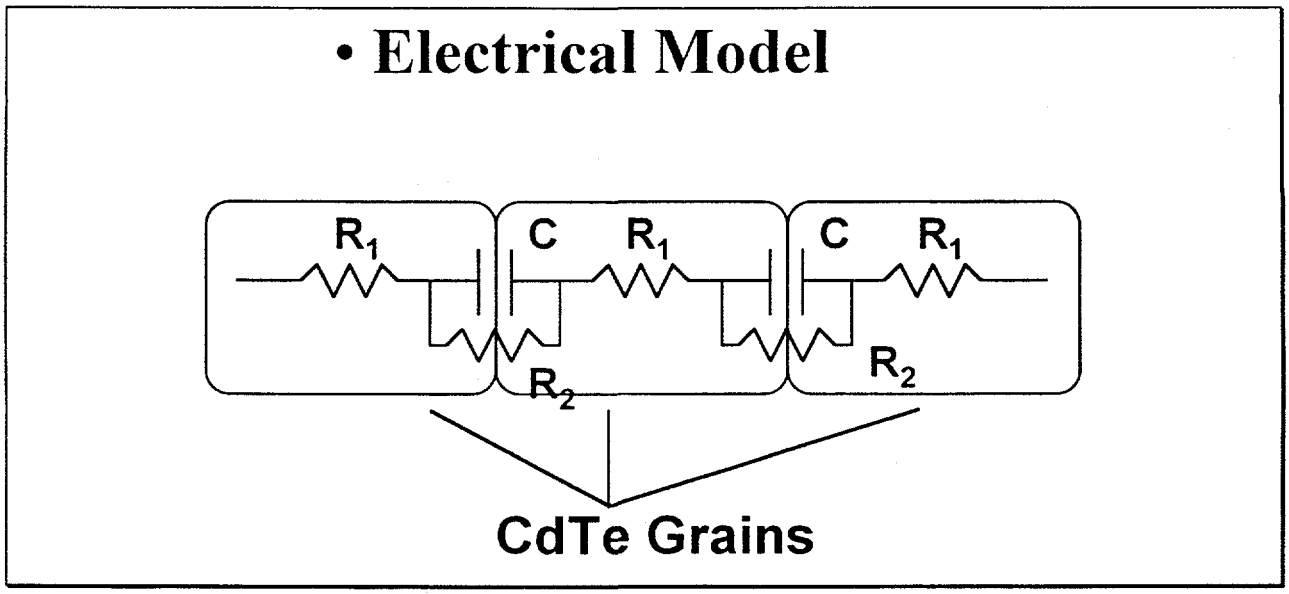

Figure 14. Model of electronic conduction through porous CdTe region based on intragrain resistance (r1) and intergrain resistance (r2) and capacitance (C).

Thus by measuring the frequency response, as shown in Figure 15., the grain-to-grain and intragrain resistances can be separated. Resistivity of the layer appears to be dominated by the grain-to-grain resistance. This is consistent with previous studies of grain boundary effects.[9] Namely, there are potential barriers for holes due to the positive charge accumulated by the boundary electronic states. The estimated "drift" barrier height varies in dark within the range 0.15-0.25 eV depending on the sample processing. Light makes this barrier lower by the amount ~0.05-0.15 eV for different samples decreasing the electrical charge at the boundary and providing much lower resistance of the inter-grain boundary which can control the resistivity of CdTe.

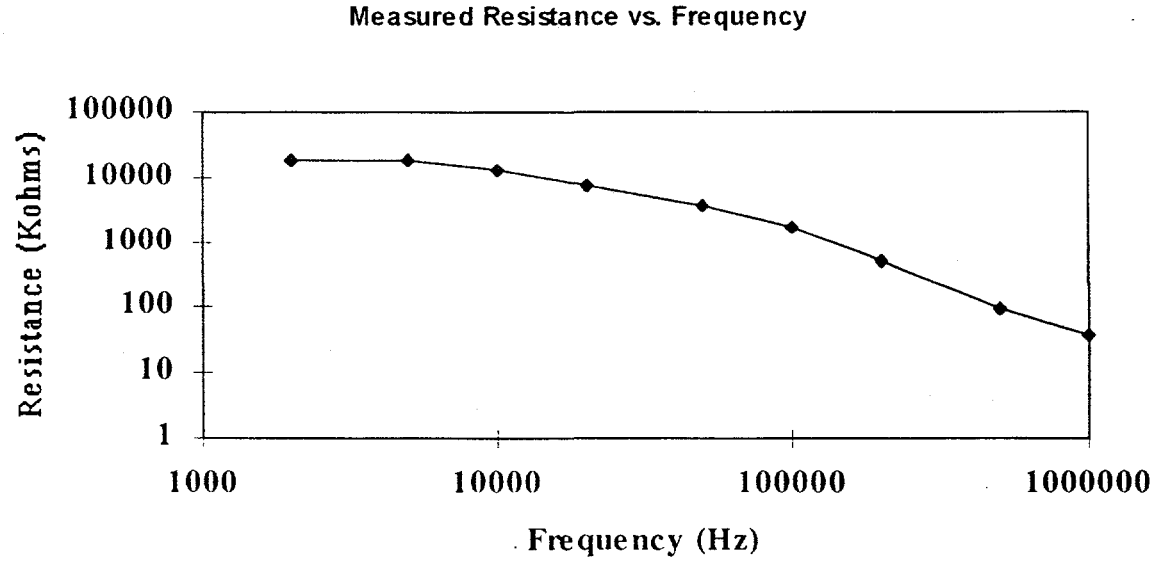

Figure 15. Measured resistance vs. frequency of porous CdTe layer.

These samples were encapsulated with feedthoughs for measuring resistance and then placed on an outdoor array for a period of time sufficient to observe instabilities in series resistance in cells. The low frequency resistances before and after exposure for different recrystallizations are presented in Table 1. These results and others with different processing indicate that with the new recrystallization procedure the CdTe sheet resistance was more stable which correlates with the series resistance changes observed in similarly prepared cells and the module data in Figure 12. above.

Recrystallization Type	Illumination	Before	After	Change(%)
Old recrystallization	dark	2.63	3.09	17
	light	0.06	0.063	5
New recrystallization	dark	3.34	3.5	5
	light	0.049	0.049	0

TABLE 2. Sheet Resistance of CdTe Layer in MW

Observation and analysis of the transition from "light" to "dark" resistance of the sample were performed. The relaxation "from light to dark" process turned out to be very slow with the instantaneous relaxation time, τ_i, increasing with time, t, almost linearly in the range of τ_i from several seconds at t~10 sec to 1,000 seconds for t~200 seconds. This result is consistent with a model supposing the presence of a high "recombination" barrier in the boundary region. This barrier decreases in light and recovers gradually after switching the light off. The restoration of recombination barrier leads to decrease of the recombination rate and increases in τ_i. The recombination barrier height estimated from these tests was almost the same for all the samples and considerably higher than the drift barrier height derived from resistance measurements themselves.

The geometry of the CdTe grain contact has been found to be critical to attaining the lowest device series resistance. Because of the morphology of the CdTe outside of GPI's depletion region are primarily through the contact of a single grain with an adjacent grain (see 2 sphere model in Fig. 13) the peripheral ring around each grain-to-grain contact is critical to conduction processes. This peripheral ring is also quite susceptible to successive treatments after the recrystallization processes. With proper treatment the majority carrier transport takes place largely through this peripheral region with a lowered drift barrier. The properties of this region as well as the hole transport through it can be affected not only by the diffusion of dopant but also by the change in crystalline structure of the outer layer of the inter-grain neck, surface impurities, or adsorbate.

Understanding the mechanism for improvement of series resistance stability due to changes in recrystallization is an important step in the improvement and maintaining control of manufacturing technology. GPI is maintaining an active effort in experimental investigation and theoretical modeling of the electronic properties of structures within our device.

3.4 CdS Thickness Measurement

To allow rapid response and control of processing conditions in a manufacturing environment, measurements of critical parameters are required by an on-line or just off-line technique. The deposition of CdS is one such process in which immediate feedback can control the average film thickness producing a reproducible output of this production step. Process control of the uniformity within a panel can also be rapidly addressed. The initial thickness of CdS determines a number of key device parameters later in the process. The diffusion of the CdS into the CdTe effects the quantum efficiency of the device at energies above the bandgap of CdS. The thicker the remaining CdS layer, the more light shorter than 520nm wavelength is absorbed in this CdS layer and, therefore, does not contribute to the photoresponse of the material. Thus, variations in the thickness of the CdS layer can directly impact the measured short circuit current in the device.

The measurement of CdS thickness can be performed by a number of optical techniques. One that is quite simple to utilize in an off-line measurement is the optical absorption of the CdS material. In this technique the intensity of the transmitted light, T, through the CdS layer follows a simple Lambert's Law model:

$$T = (1-R)\exp(-\alpha * t)$$

where R is the reflected light, α is the absorption coefficient and the thickness, t, of the CdS layer. With the assistance of NREL staff the absorption coefficient of our CdS layer at the wavelength of interest was determined. The transmission of the CdS films is shown in Figure 16. as a function of thickness determined by an alternate method and shows a 98% correlation between the two parameters. By utilizing appropriate blanks and corrections for additional reflections when the CdS is added, a measurement representative of the thickness can be obtained. However, trends in CdS thickness over the period of a manufacturing run can be easily determined with only initial transmission measurements.

Error! Not a valid embedded object.

Figure 16. Transmitted power vs. CdS thickness (points_ and the exponential fit (line).

3.5 Dopant Incorporation

The method for the addition of dopant to the device was modified over the past year. The new method was tested by a number of techniques for initial efficiency and stability. One stability test that was performed involved the heating of small cell devices in nitrogen at 65°C for 1900 hours. The test was carried out as a function of dopant concentration and the results are shown in Figure 17. The stability rises to a maximum as a function of concentration followed by a steep drop off at higher concentration. The specific concentration where the maximum occurs is dependent on many parameters involving the condition of the CdTe substrate material as well as the incorporation technique of the dopant. The loss of efficiency on either side of the maximum appears to come from increases in the series resistance. The short circuit current and open circuit

voltage change is very small and does not correlate with the observed loss. The result of this study has allowed us to understand dopant effect on our present morphology and directed us in the understanding of possible degradation mechanisms.

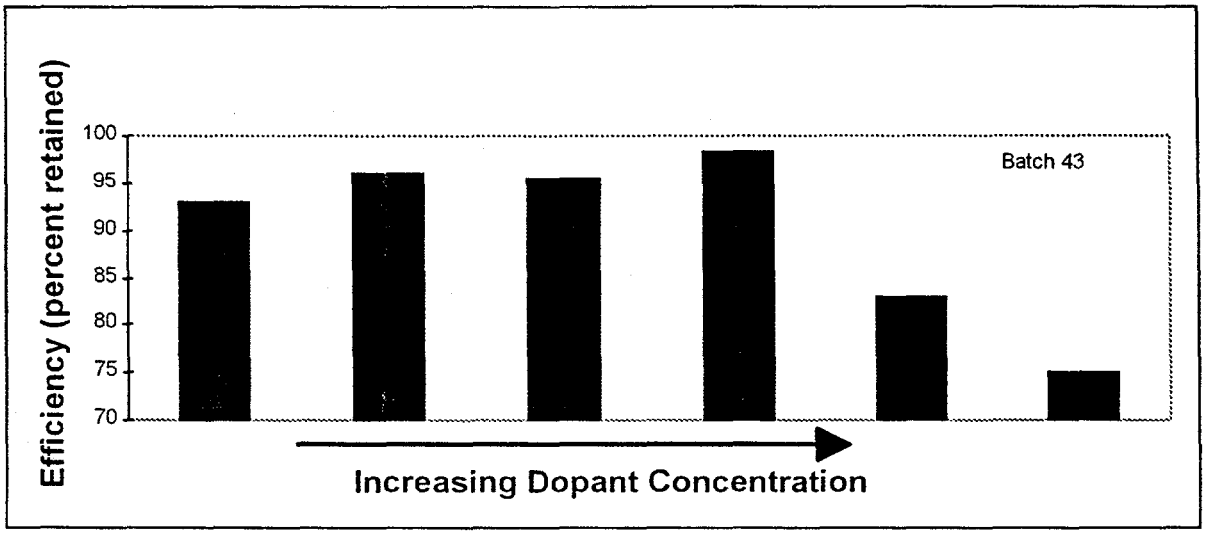

Figure 17. Efficiency of CdTe cells as a function of dopant concentration after 1400 hours in 65°C in the dark.

3.6 Diffusion of Sulfur

In the CdTe/CdS system the limits of current collection are bounded by the bandgap of CdTe near 850 nm and the absorption by CdS on the ultraviolet end of the spectrum. The absorption in CdS can produce a strong reduction in the spectral response above the band edge near 520nm. The spectral region above this edge accounts for 23% of the total available current. One of the keys to high current collection in this system is through the reduction of CdS thickness. However recent work has shown that reduction in the thickness of CdS layers generally has produced a lower Voc as the thickness of CdS is reduced below about 750 Angstroms.(ref Sites IEEE p.853) At CdS thicknesses of 400 Ang. the spectral response curves show no current loss due to absorption of CdS below 500 nm. While the explanation for reduction in Voc has not been verified, there is some belief that it is associated with passivation within the junction region.

Recent studies at GPI have shown that Voc levels near 800 mV can be obtained with very thin CdS layers. The small cell spectral response in Figure 2. indicates a CdS layer close to 400 Ang by comparison with spectra in reference 18. This level of CdS is substantially lower than the level that was originally deposited. The reduction in CdS level is due to interdiffusion with CdTe during the recrystallization process. The interdiffusion is demonstrated by electron microprobe (EPMA) studies of a cross section of a device shown in Figure 18. This shows the measurement Cd, Te, and S from the glass substrate on the left hand side of the figure to the back surface on the right. The influence of topography is indicated by the variation of signal intensity of the Cd and Te within the middle of the region where there should be none. The sulfur variation is shown in the bottom of this figure has the same spatial expansion as the Cd and Te. The figure indicates that sulfur is widely dispersed over the entire thickness of the CdTe region. The spatial

sensitivity of EPMA is not fine enough to determine whether the increased CdS concentration near its original location is in a thin layer or dispersed as indicated by the probe results.

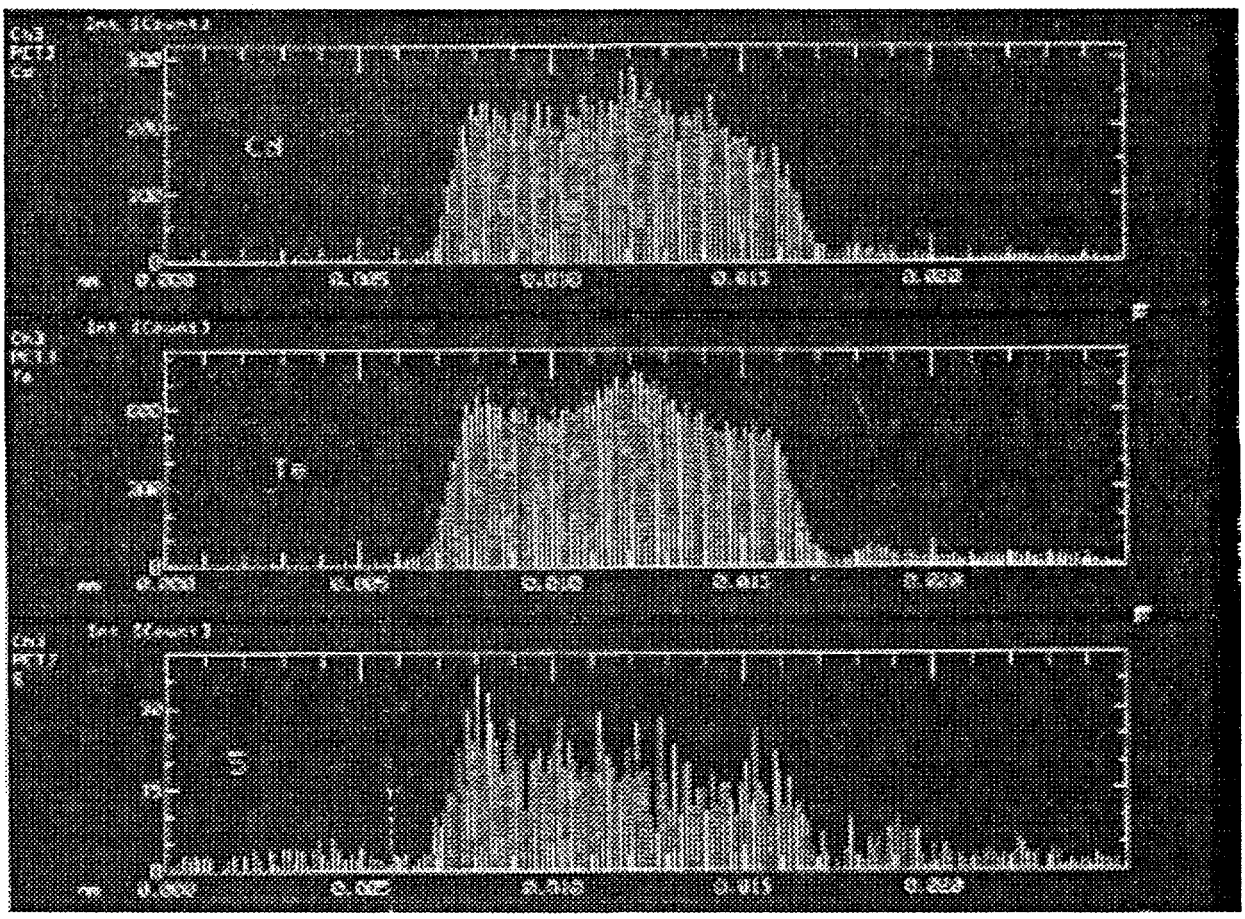

Figure 18. Electron microprobe of a cross section of a GPI cell, soda lime glass is on the left and graphite electrode on the right for Cd, Te, and S. Thickness of the material is approximately 10 microns.

Thus the diffusion of CdS leads to a reduction of the original thickness, reduction in absorption, and higher current collection efficiency of the device. Studies are continuing to evaluate the uniformity of the remaining layer of CdS.

3.7 Back Contact

The ability to make high quality and stable electrical contacts with CdTe is a critical issue for module development. One of the common materials used for contacting is graphite. The application process of graphite to CdTe typically involves a heat treatment process to produce the lowest series resistance. A study was carried out to investigate the resistivity of the graphite used at GPI as a function of its heat treatment temperature and the results are shown in Figure 19. The points indicate the sheet resistance of the graphite before and after the heat treatment process. The decrease in resistivity is as a function of temperature indicates the necessary processing required to optimize the graphite resistance of our device. The mechanism for the

improvement is not known, however, the improved conductivity could arise from the continued removal of a solvent used in application and densification of the graphite layers producing better grain to grain contact.

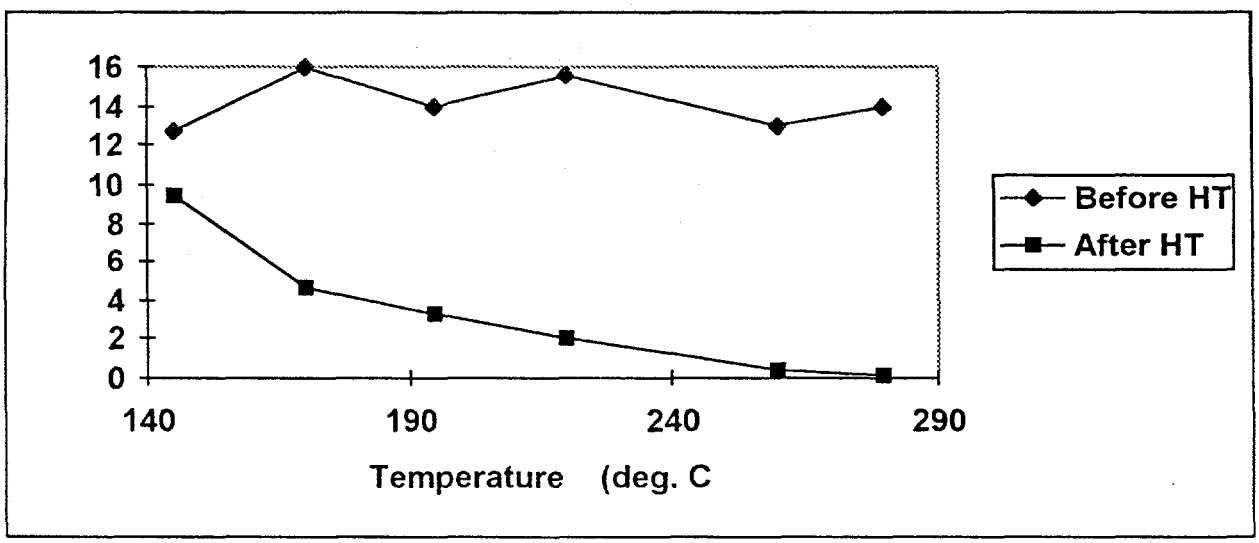

Figure 19. Graphite sheet resistance before (diamond) and after (square) different heat treatment temperatures.

4.0 Conclusions and Future Work

It is clear that significant progress has been made in the manufacture of CdTe modules by the narrowing of the gap between efficiency of small cells (approx. 13%) and efficiency of the active area of our panels (greater than 10%). This increase is due to a combination of improvements in morphology, the material properties, and improvements in uniformity of the 2' x 2' panels. These improvements in uniformity and reproducibility within panels, within batches, and batch to batch indicate the substantial increase in control of the manufacturing process. An example of the improvement in reproducibility and uniformity is evidenced by control of the CdS deposition process. In addition, this increase in reproducibility allows the separation of results in parametric studies to be carried out with much less fluctuations in results. Other process improvements that have led to efficiency and stability increases include the incorporation of the different dopants and the technique of incorporation. The improvements in module design and encapsulation continue to lead us to more cost competitive module production.

These improvements in panel and cell efficiency have come about by a greater understanding of the effect of process steps on the electronic properties of the material. Clearly, the changes in CdTe morphology brought about by the changes in the recrystallization process led to dramatic increases in efficiency and stability of the material. These changes were manifested in the improvements in the junction properties of the material, both in the increase in spectral response and uniformity of response on the microscopic scale. The changes in recrystallization also led to the realization of the importance of including grain boundary contributions to our model.

Future work will continue to include a combination approach of process improvement with a concomitant attempt to understand the role of these changes on the electronic properties of the material. We will continue to focus on the effects of morphology on electronic properties. The morphology is obviously a controlling factor in the transport control of impurities and dopants. The migration of these materials both within the junction region and in the porous region of the material are believed to be important in the position and width of the junction region. Additional work is being carried out on the effects of the porous region of our material and its effect on efficiency and stability. The work on the porous region of our CdTe layer will be carried out in conjunction with work on improvement of the back contact to the CdTe layer.

Additionally, after the period that this report covered, several world record efficiencies have been produced by GPI and are included here for clarity and completion.

First, a 14.7% efficiency device measuring ~0.3 cm^2 was confirmed at NREL as a world record CdTe efficiency on soda-lime glass substrate.

Second, numerous 61cm x 61cm modules have been produced by GPI. NREL has confirmed a 31.0W module with total area of 3794cm^2 (8.2% Eff.), an aperture area of 3366cm^2 (9.2% Eff.), and an active area of 2777cm^2 (11.2% Eff.).

References

1. S. Albright and J. Kester, "Module Process Optimization and Device Efficiency Improvement for Stable, Low-Cost, Large-Area Cadmium Telluride-based Photovoltaic Module Production" Final Technical Progress Report for subcontract ZN-9-19019, (1996).

2. S.P. Albright, R. Chamberlin, B. Ackerman, and J. F. Jordon, "Performance Measurement irregularities on CdS/CdTe Devices and Modules", Int. J. Solar Energy, 12, 109-120, (1992).

3. Ken Zweibel, Harin S. Ullal, Bulko von Roedern, " Progress and Issues in Polycrystalline Thin-Film PV Technologies", in 24th IEEE Photovoltaic Specialists Conference,pp. 745-750, (1996).

4. J. Jordan and S. Albright, "Photovoltaic Cell with Thin CdS Layer", Patent Number 5279678, (1994).

5. J. Jordan "Photovoltaic Cell and Method", Patent Number 5261968 (1993).

6. R.A. Sasala, J. Bohland and K. Smigielski, "Physical and Chemical Pathways for Economic Recycling of Cadmium Telluride Thin film Photovoltaic Modules," in the 24th IEEE Photovoltaic Specialist Conference, pp. 865-868 (1996).

7 W.D. Kingery and M.Berg, "Study of the Initial Stages of Sintering Solids by Viscous Flow, Evaporation-Condensation, and Self Diffusion", Jour. Applied Phys., 26,1205-1212 (1955).

8. T. Quadir and D.W. Ready, "Microstructure Development of Zinc Oxide in Hydrogen", J. Am. Ceram. Soc., 72(2) 297-302 (1989).

9. Thorpe, T.P., Fahrenbruch A.L., and Bube R.H., J. Appl. Phys. 60, 3666 (1986).

10. J.E. Granata, J.R. Sites, G. Contreras-Puente, and A. C. Campaan, Effect of CdS Thickness on CdS/CdTe Quantum Efficiency", in the 24th IEEE Photovoltaic Specialist Conference, pp. 853-856 (1996).

REPORT DOCUMENTATION PAGE

Form Approved
OMB NO. 0704-0188

1. AGENCY USE ONLY (Leave blank)	2. REPORT DATE	3. REPORT TYPE AND DATES COVERED
	July 1997	Annual Technical Progress Report, 1 September 1995 - 31 August 1996

4. TITLE AND SUBTITLE

The Improvement of Near-Term CdTe Processing and Product Capabilities and Establishment of Next-Generation CdTe Technology; Annual Technical Progress Report, Phase One, 1 September 1995 - 31 August 1996

5. FUNDING NUMBERS

C: ZAF-5-14142-06
TA: PV704401

6. AUTHOR(S)

J. Kester and S. Albright

7. PERFORMING ORGANIZATION NAME(S) AND ADDRESS(ES)

Golden Photon, Inc.
4545 McIntyre St.
Golden, CO 80403

8. PERFORMING ORGANIZATION REPORT NUMBER

9. SPONSORING/MONITORING AGENCY NAME(S) AND ADDRESS(ES)

National Renewable Energy Laboratory
1617 Cole Blvd.
Golden, CO 80401-3393

10. SPONSORING/MONITORING AGENCY REPORT NUMBER

SR-520-23262

11. SUPPLEMENTARY NOTES

NREL Technical Monitor: H.S. Ullal

12a. DISTRIBUTION/AVAILABILITY STATEMENT

12b. DISTRIBUTION CODE

UC-1263

13. ABSTRACT *(Maximum 200 words)*

This report describes the accomplishments of Golden Photon, Inc. (GPI) during Phase One of this subcontract. GPI researchers demonstrated a 29.3-watt, 2-ft. x 2-ft. module aperture-area efficiency of 8.8%, with an active-area efficiency of 10.5%; improved CdTe morphology through recrystallization demonstrated by efficiency and stability; reduced production costs by reduced weight, thickness of module, and permeability to water; modified graphite and dopant incorporation, which resulted in greater efficiency, uniformity, and reproducibility; participated in team efforts to provide samples for CdS thickness/V_{oc} testing, distribute CdTe material for back contact, and develop performance certification standardization; and provided efficiency and life-testing data modules to the National Renewable Energy Laboratory.

14. TERMS

photovoltaics ; cadmium telluride ; CdTe processing ; thin films ; module fabrication ; next-generation technology

15. NUMBER OF PAGES
36

16. PRICE CODE

17. SECURITY CLASSIFICATION OF REPORT	18. SECURITY CLASSIFICATION OF THIS PAGE	19. SECURITY CLASSIFICATION OF ABSTRACT	20. LIMITATION OF ABSTRACT
Unclassified	Unclassified	Unclassified	UL